

# Environmental Science Processes & Impacts

Accepted Manuscript



This is an *Accepted Manuscript*, which has been through the Royal Society of Chemistry peer review process and has been accepted for publication.

*Accepted Manuscripts* are published online shortly after acceptance, before technical editing, formatting and proof reading. Using this free service, authors can make their results available to the community, in citable form, before we publish the edited article. We will replace this *Accepted Manuscript* with the edited and formatted *Advance Article* as soon as it is available.

You can find more information about *Accepted Manuscripts* in the [Information for Authors](#).

Please note that technical editing may introduce minor changes to the text and/or graphics, which may alter content. The journal's standard [Terms & Conditions](#) and the [Ethical guidelines](#) still apply. In no event shall the Royal Society of Chemistry be held responsible for any errors or omissions in this *Accepted Manuscript* or any consequences arising from the use of any information it contains.



[rsc.li/process-impacts](http://rsc.li/process-impacts)

## Environmental impact

In this paper we describe a new laboratory setup to study the response of volatile plant emissions to different types of environmental stress. The centerpiece is the combination of two plant chambers with a reaction chamber that allows for photochemical processing of the plant emissions. Modern analytical tools such as proton-transfer-reaction time-of-flight mass spectrometry and gas chromatography allow for fast, precise and detailed chemical analysis. Results from a pilot study demonstrate the capacity of the system to investigate environmental issues of high importance, such as the discrepancy between the observed and predicted chemical loss of ozone via reactions with plant emissions; the impact of pollution and UV-B radiation on plant emissions.

## A plant chamber system with downstream reaction chamber to study the effects of pollution on biogenic emissions

Cite this: DOI: 10.1039/x0xx00000x

Received 00th January 2012,  
Accepted 00th January 2012

DOI: 10.1039/x0xx00000x

www.rsc.org/

J. Timkovsky<sup>a</sup>, P. Gankema<sup>b</sup>, R. Pierik<sup>b</sup> and R. Holzinger<sup>a</sup>,

A system of two plant chambers and a downstream reaction chamber has been set up to investigate the emission of biogenic volatile organic compounds (BVOCs) and possible effects of pollutants such as ozone. The system can be used to compare BVOC emissions from two sets of differently treated plants, or to study the photochemistry of real plant emissions under polluted conditions without exposing the plants to pollutants. The main analytical tool is a proton-transfer-reaction time-of-flight mass spectrometer (PTR-TOF-MS) which allows online monitoring of biogenic emissions and chemical degradation products. The identification of BVOCs and their oxidation products is aided by cryogenic trapping and subsequent in situ gas chromatographic analysis.

### Introduction

Volatile organic compounds (VOCs) are reactive substances in the atmosphere which have a strong impact on atmospheric chemistry.<sup>1,2,3</sup> Biogenic volatile organic compound (BVOC) emissions constitute approximately 90% of global VOC emissions which are estimated to be ~1150 Tg C/year.<sup>4</sup> Oxidation of BVOCs in the atmosphere in the presence of NO<sub>x</sub> leads to the formation of ozone. Tropospheric ozone is a greenhouse gas and a strong oxidant which makes it harmful for living organisms.<sup>5,6</sup> Moreover, oxidation products of BVOCs contribute to secondary organic aerosol (SOA) formation through condensation on existing particles or the formation of new particles.<sup>7,8</sup> Aerosols and ozone can penetrate into the lungs of humans thus causing long- and short-term health effects.<sup>9</sup> Furthermore, aerosols and ozone have an impact on Earth's climate: ozone is a strong greenhouse gas and aerosols scatter and/or absorb solar radiation. Aerosols also influence the climate indirectly by serving as cloud-condensation nuclei.<sup>10</sup> While BVOCs are known to affect the atmosphere, much remains unknown about how atmospheric pollutants affect plant VOC emissions. Increased ozone levels may increase or decrease BVOC emissions, depending on plant species and environmental conditions. For example, Beauchamp et al.<sup>11</sup> showed that C<sub>6</sub>-volatile emissions increased after acute ozone exposure in tobacco plants, while Hartikainen et al.<sup>12</sup> showed decreased VOC emissions upon elevated ozone levels in birch

trees. In addition, Karl et al.<sup>13</sup> showed that pollutants like oxygenated VOCs can be removed by plants through dry deposition. At the same time it is not understood how such deposition influences the ability of plants to emit BVOCs.<sup>13</sup> Plant VOC emissions are affected by many environmental factors, including abiotic factors like temperature and light as well as biotic factors like herbivores, pathogens and neighboring plants.<sup>14-17</sup> Here we present a setup of plant chambers and a reaction chamber, which can be used to study interactions between BVOC emissions and pollution. A similar setup has been described by.<sup>18</sup> Their facility is much larger (it uses trees rather than small potted plants) and optimized to simulate natural conditions. The smaller laboratory based setup that we describe here is flexible and adaptable to study specific processes at the plant level and represents an intermediate between the large facility described by Mentel et al.<sup>18</sup> and a much simpler setup such as used by Karl et al.<sup>19</sup> The main features include automated operation to study real plant emissions under different environmental conditions. BVOC analysis is based on proton-transfer-reaction time-of-flight mass spectrometry (PTR-TOF-MS) which allows precise online measurements of different VOCs in the air with high mass resolution.<sup>20,21</sup> In addition, the PTR-TOF-MS is coupled to a gas chromatograph (GC) system in order to improve the identification of isomers (e.g. different monoterpenes). Results from an ozonolysis experiment with  $\beta$ -pinene and three experiments with birch (*Betula pendula*) seedlings (referred to

as experiment A, B, and C) are shown here as an example to demonstrate the performance of the system.

## Description of the setup

The schematic setup of the system is shown in Fig. 1. Two optional chamber setups are shown in panels A and B. Fig. 1C shows how the PTR-TOF-MS is connected to the different sampling ports of the chamber system, and Fig. 1D shows the functioning of the GC system.

## The plant and reaction chambers

Two types of plant chambers are available for experiments. Their internal volumes are 25 L and 785 mL, and we refer to them as large plant chamber and small plant chamber, respectively.

As large plant chambers we use two glass desiccators, each consisting of three parts: the cap, the desiccator body and the hose, which is located in the cap. The hose has a long outlet ( $l = 25$  cm, ID = 9 mm), which is directed towards the bottom of the desiccator and allows sampling from the center of the plant chamber. The gas inlet to the chamber is located at the top of the hose.

The small plant chambers are custom built and consist of a glass cylinder (inner diameter 100 mm, height 100 mm), a glass lid and a dividable Teflon (PFTE) bottom plate sealed with spring clamps and Teflon coated O-rings. For UV-B treatment, we use a lid with 2 mm thick quartz glass and a broad spectrum UV-B lamp (UV21, 9 W, Waldmann, The Netherlands) at adjustable height above the plant chamber. The bottom plate has a 2 mm hole in the middle that fits around the stem of an individual plant, allowing measuring shoot emissions only. Inlet and outlet (inner diameter 18 mm) are positioned opposite each other 40 mm above the bottom of the chamber.

The custom-made reaction chamber is made from perfluoroalkoxy film (PFA, thickness 0.05 mm, HP Products, the Netherlands) and has a cylindrical shape. The walls were sealed by welding the PFA film with a heat gun (Steinel, Germany). The physical characteristics of the reaction chamber are the following: diameter = 45 cm, height = 50 cm, volume = 80 L. The bottom of the chamber is fixed to a ground plate covered with a PFA film. The axle of a polytetrafluoroethylene ventilator (PTFE, OD = 10 mm, Bola, Germany) is lead through the center of the ground plate, the ventilator is positioned in the center of the chamber. Operating the ventilator at 2 Hz keeps the chamber well mixed during experiments. All mounting parts in contact with the air inside the reaction chamber were made from Teflon (PTFE). The tightness of the reaction chamber was tested by filling the chamber with acetone at levels of  $\sim 350$  nmol/mol and monitoring the mixing ratio without gas flow through the chamber. No significant leaks were detected.

The flow through the large plant chambers can be controlled by thermal mass-flow controllers (MKS Instruments, Germany) in the range 0-20 and 0-5 standard L/min (standard is referring to standard conditions: 1013.25 hPa, 273.15 K) for chamber 1 and 2, respectively. The flow through the small plant chambers can be also controlled by thermal mass-flow controllers (MKS Instruments, Germany) in the range 0-2 standard L/min. Although we operated the chambers without active mixing, tests showed that there was sufficient convection to completely mix the air inside the large plant chambers in less than 30 minutes (see section 'Mixing in the plant chambers'), even at

flow rates as low as 2.5 L/min (10 min residence time). We used pressurized (5 bars) ambient air which was purified through a custom made charcoal filter. The charcoal was cleaned once a week by removing the charcoal from the tube and placing it overnight in an oven at 160 °C.

In the 'dual plant chamber' setup (Fig. 1A) the sampling ports are located directly at the outlets of the plant chambers and a third sampling port is located after the charcoal filter to monitor the incoming air. The elements of the system drawn in dashed line boxes are optional elements. The ozone generator can be used for studies with large plant chambers, whereas UV-B lamp can be used for studies with small plant chambers. In the 'reaction chamber' setup (Fig. 1B) the sampling ports are located directly after the reaction chamber, after the plant chambers, and after the charcoal filter. Relative humidity and temperature sensors (HMP 60, Vaisala, Finland) are located at the outlets to monitor humidity and temperature in all chambers.

We use Teflon (PFA) tubing to connect the large plant chambers, the reaction chamber, and instruments (length between plant and reaction chamber = 145 cm, ID = 9 mm). Defined amounts of ozone can be added before large plant chamber 1 (Fig. 1A) or the reaction chamber (Fig. 1B) with an ozone generator (Model 49i-PS, Thermo Scientific, US). This is done by turning on the generator (set to 1500 nmol/mol) and switching valve 3. The ozone addition to the large plant chamber 1 and the reaction chamber is controlled with a thermal mass-flow controller (MKS, Germany) in the range 0-2 L/min. Ozone is monitored (O3 analyzer model 49 W003, Thermo Environmental Instruments Inc., USA) at the outlet of either the large plant chamber 1 or the reaction chamber.

An array of nine 36W/840 TL-D lamps (Philips, the Netherlands) above the plant chambers is used to produce light levels of 130-150  $\mu\text{mol}/\text{m}^2/\text{s}$  photosynthetically active radiation (PAR:  $\lambda = 400$ -700 nm) at leaf level inside the large plant chambers when the lid was closed. These light levels are within the range used by previous plant emission studies<sup>17,22-24</sup> and are common to plant growth chambers. A practical advantage of using light at these intensities is that we do not encounter significant heating in the large plant chambers and therefore active cooling is not required.

## Analytical tools

### PTR-TOF-MS

Fig. 1C shows how the PTR-TOF-MS is switched between the three sampling ports of the chamber system, the effluent of the GC column (the PTR-TOF-MS is also used as detector for the GC system), and laboratory air, which can be routinely monitored as well. This valve system is implemented with 1/8" PFA tubing, four 2-way and two 3-way Teflon (PFA) solenoid valves (TEQCOM, port size 1/8", orifice 0.125). We use a commercial PTR-TOF 8000 instrument (Ionicon Analytik GmbH, Austria), which has been described by Jordan et al.,<sup>20</sup> with the following parameters: temperature of the drift tube, 60 °C; temperature of the inlet tube, 60 °C; drift tube pressure, 2.15 hPa; ion source voltages,  $U_s = 140$  V,  $U_{so} = 92$  V; ratio of the applied to the drift tube voltage and the number of molecules in the drift tube, E/N, 134 Td; extraction voltage at the end of the drift tube,  $U_{dx} = 35$  V. The ion source current is kept between 5 and 7 mA and we provide a water flow of 4 mL/min to the ion source. At normal operational conditions the intensity of the primary signal  $\text{H}_3\text{O}^+$  (detected at  $m/z$  21.023 as  $\text{H}_3^{18}\text{O}^+$ ) is around  $2.5 \cdot 10^5$ - $1 \cdot 10^6$  cps. However, during experiments B and C the primary signal was low ( $\sim 5 \cdot 10^4$ - $1 \cdot 10^5$  cps), whereas

during experiment A the primary signal was at its normal level ( $\sim 2.5 \times 10^5$  cps). During the ozonolysis of  $\beta$ -pinene experiment the primary signal was  $\sim 1 \times 10^5$  cps. The ratios of the intensities  $I(\text{O}_2^+)/I(\text{H}_3\text{O}^+)$ ,  $I(\text{NO}^+)/I(\text{H}_3\text{O}^+)$  and  $I(\text{H}_3\text{O}(\text{H}_2\text{O})^+)/I(\text{H}_3\text{O}^+)$  were less than 0.02, less than 0.003 and less than 0.25.

The settings of the TOF are such that every 60 microseconds a pulse of ions is injected into the mass spectrometer, which corresponds to a mass range of 0-1157 Th. 16667 of these initial mass spectra are averaged and saved to one mass scan which corresponds to a time resolution of one second. The mass resolution ( $m/\Delta m$ , where  $\Delta m$  is the full width at half maximum) is typically in the range of 3500-5000. Data processing is done with Interactive Data Language (IDL, version 7.0.0, ITT Visual Information Solutions), using custom made routines described by Holzinger et al. (2010).<sup>25</sup>

Mixing ratios of most compounds were calculated according to the method described in Holzinger et al.,<sup>26</sup> which involves the use of default reaction rate constants ( $3 \times 10^{-9} \text{ cm}^3 \text{ s}^{-1} \text{ molecule}^{-1}$ ), default transmission efficiencies, and calculated reaction times. The accuracy of the calculated mixing ratios should be better than 50% for most compounds limited by the uncertainty in the used default reaction rate constant.<sup>26</sup> In addition, a commercially available calibration mixture (Apel-Riemer Environmental, Inc.) was used to calibrate the mixing ratios of monoterpenes, acetaldehyde and acetone with an accuracy of 17%, calculated as the sum of the precision of PTR-TOF-MS and the accuracy of the gravimetrically mixed calibration standard.

The mixing ratios of monoterpenes were calculated as the sum of the signals detected at  $m/z$  81.069 and  $m/z$  137.133 for experiments with pure compounds (here  $\beta$ -pinene). However, we found that in experiments with biogenic emissions other compounds were also detected at  $m/z$  81.069 (C6 alcohols or aldehydes). Calibration experiments with a gas standard containing  $\alpha$ -pinene showed that 32% of the total amount of the monoterpene was found at  $m/z$  137.133. Thus, for the experiments with biogenic emissions, mixing ratios of monoterpenes were calculated by multiplying the signal detected at  $m/z$  137.133 by a calibration factor of 3.13.

### GC system with VOCs cryogenic trapping

The GC system features two cryogenic traps that can be electrically heated with resistance wire and submerged into liquid nitrogen by pneumatic lifters. The sampling line (1/8" PFA) is connected (port 5 in Fig. 1C and D) downstream of the two 3-way valves that connect the PTR-TOF-MS to the sampling ports of the chamber system. This ensures that GC-sampling and online monitoring with the PTR-TOF-MS occurs at the same time. The primary sampling trap is a W-shaped 1/8" stainless steel tube (ID = 1.5 mm) with sulfinert coating (Restek Inc.) which is connected with 1/16" PEEK tubing to a 6-port stainless steel Valco valve (sulfinert coating). A needle valve before the trap is used to regulate the sampling flow and ensures that sampling is at low pressure ( $\sim 200$  hPa) to prevent condensation of oxygen. The collection efficiency has been tested for  $\alpha$ -pinene, methanol and toluene to be close to 100% for sampling flows up to 35 mL/min. During operation the trap is pre-cooled for 5 minutes before sampling. We use a sampling flow of 30 mL/min which is measured with a thermal mass-flow meter (MKS Instruments, Germany) and maintained with a membrane pump (Vacuubrand GmbH, Germany) downstream of the sampling trap.

Switching the 6-port valve allows transferring the sample to the focusing trap, which consists of a U-shape 1/8" stainless steel

tube with a glass capillary through it (ID = 320  $\mu\text{m}$ , SGE Analytical Science, Australia). The sample is released by heating the sampling trap to 100  $^\circ\text{C}$  within 2 minutes. A helium flow (ultrapure He, Air products) of 2 mL/min is used to transfer the sample to the focusing trap. Typically a period of 10 minutes is allowed to complete the transfer, which corresponds to a gas volume 5 times the internal volume of the sampling trap, the focusing trap and the transfer lines. Immediately thereafter the 6-port valve is switched back and the sample is injected into the GC column while the effluent is monitored with the PTR-TOF-MS. Injection is achieved by heating the focusing trap to 200  $^\circ\text{C}$  within 75 seconds. In general, a two cryotrap system is advantageous because better peak shape can be achieved and the reduced amount of water in the sample prolongs the lifetime of the GC column. The first cryotrap allowed for the initial sampling of VOCs. The second cryotrap was used to focus the presampled VOCs in a much smaller volume, allowing for a much quicker transfer of the VOCs from the cryotrap to the GC column. The amount of water in the sample transferred to the second cryotrap was reduced by  $\sim 90\%$  via condensing on the line/Swagelok union located downstream of the sampling cryotrap. This water was removed from the system during the consecutive sampling step. For the chromatography we use a 30 m DB-5MS column (ID = 0.25 mm, film thickness = 0.25  $\mu\text{m}$ ) with He as a carrier gas (2 mL/min, controlled with 20 mL/min thermal mass-flow controller, MKS Instruments, Germany). After injection the column is kept at 40  $^\circ\text{C}$  for one minute, heated to 150  $^\circ\text{C}$  at 5  $^\circ\text{C}/\text{min}$  and then to 250  $^\circ\text{C}$  at 20  $^\circ\text{C}/\text{min}$ .

For analysis the effluent of the GC column is diluted with 38 mL/min of nitrogen (ultrapure nitrogen, 5.7 purity, Air products), which is achieved by providing excess nitrogen and setting the flow into the PTR-TOF-MS to 40 mL/min (Fig. 1D). The mixture of effluent and nitrogen is transferred through 1/8" PFA line to port 6 (Fig. 1C and D).

### Automation and control system

Valve positions, flows, cryotrap positions, temperatures and other elements are automatically operated with a controlling set (National Instruments NI cDAQ-9178) that can be programmed in Labview's (LabVIEW 2011, National Instruments) user-friendly interface. Control sequences are created as simple text documents containing the commands for valve positions, set temperatures, etc.

The values of the elements underlined red in Fig. 1 are saved to an engineering log together with other parameters such as time, ozone mixing ratios in the reaction chamber, set value of ozone generator, sampling and focusing cryotrap temperatures, and temperature in the GC oven. These data are recorded every second to fit the time resolution of the PTR-TOF-MS.

### Operation of the system

To demonstrate the operation of the system, Fig. 2 shows the course of the mixing ratios detected at  $m/z$  81.069 ( $\text{C}_6\text{H}_9^+$  fragment) for one cycle of experiment A. The PTR-TOF-MS was switched between the different ports to measure as follows (see Fig. 2): for 10 minutes reaction chamber air, for 5 minutes purified air, for 10 minutes large plant chambers air, for 25.5 minutes GC effluent, for 10 minutes large plant chambers air, for 36 minutes reaction chamber air (ozone addition to the reaction chamber happens during this period), for 25.5 minutes GC effluent, for 5 minutes lab air. Thereafter, new two-hour cycles were started automatically.

The periods of GC sampling (7 minutes each) are also indicated in Fig. 2. Ozone addition lasted for 17 minutes (see blue bracket in Fig. 2) and GC sampling was performed during the last 7 minutes of the ozone treatment.

The following periods (indicated in Fig. 2 by the respective lines below the x-axis) were used for averaging/integration: last 7 minutes of non-ozonated reaction chamber air measurements, last 4 minutes of purified air measurements, last 9 minutes of first large plant chamber air measurements, first 15 minutes of first GC chromatogram, last 4 minutes of second large plant chamber air measurements, last 7 minutes of ozonated reaction chamber air measurements, first 15 minutes of second GC chromatogram.

During the experiment with small plant chambers, the PTR-TOF-MS was switched between the different ports to measure as follows: for 6 minutes small plant chamber 1 air, for 6 minutes small plant chamber 2 air, for 5 minutes purified air, for 5 minutes lab air. Thereafter, a new cycle was started automatically.

## System performance

### Mixing in the plant chambers

An experiment to test mixing of air in the large plant chambers was conducted: flow through the empty plant chamber was maintained at 2.5 L/min and contained ~45 nmol/mol of limonene. The flow was produced by diluting a small flow (standard 1 mL/min) of headspace air from a flask with liquid limonene (Sigma Aldrich, 98%) into the larger flow of purified air. The mixing ratios were measured in the middle and at the bottom corner of the plant chamber with the PTR-TOF-MS and were equal to the incoming limonene mixing ratio after ~30 min. This indicated that the mixing in the plant chambers was as expected and sufficient for the experiments presented here.

### VOCs transfer between the large plant chambers and the reaction chamber

Fig. 3 presents online data (experiment B) of the large plant chambers and the reaction chamber without ozone addition. In general, there is good agreement between the mixing ratios in the reaction chamber and the large plant chambers for most compounds. However, for monoterpene and  $m/z$  85.064 (corresponding to the molecular formula  $C_5H_9O^+$ ) the mixing ratios were somewhat lower in the reaction chamber compared to the large plant chamber. This was likely caused by the fact that equilibrium was not yet completely reached by the time when reaction chamber measurements were performed after the preceding ozone addition to the reaction chamber (time difference was less than 3 residence times equal to 34.5 minutes). For  $m/z$  69.070 and 71.049 in some cases lower mixing ratios were observed in the large plant chambers. This might be caused by contamination from the reaction chamber walls.

### GC system

Example chromatograms obtained during experiment A are shown in Fig. 4. The five labeled peaks in panel C (Fig. 4) are attributed to a C6-leaf alcohol or aldehyde, 2-hexenal,  $\alpha$ -pinene, d-limonene and  $\beta$ -phellandrene. The attribution is done based on the presence of other ions with the same retention times in combination with retention times database,<sup>27</sup> performed calibration measurements and previous studies.<sup>28</sup> Two little

peaks observed after  $\alpha$ -pinene and d-limonene are not identified.

A crucial point of the GC/PTR-TOF-MS system is the quantitative correspondence between GC and online measurements. Equation 1 defines the recovery factor (RF) as the ratio between the amount of substance of a VOC measured with the GC setup ( $n(\text{VOC})_{\text{GC}}$ ) versus the amount of substance sampled ( $n(\text{VOC})_{\text{sampled}}$ ). The former was calculated by integrating the GC peak(s) at a particular  $m/z$  value, the latter was calculated from the online measured mixing ratio at the same  $m/z$  during the time of sampling and the sampled volume:

$$RF = \frac{n(\text{VOC})_{\text{GC}}}{n(\text{VOC})_{\text{sampled}}} \quad (1)$$

In Table 1 we present recovery factors of several compounds based on experiments A, B and C. To calculate the recovery factors no background was subtracted from the measured signal. The obtained recovery factors are in the range 0.71 - 1.38 indicating a reasonable agreement between online and GC measurements. Deviations from unity are most likely due to different levels of instrumental background during the online and GC effluent measurements. Also, there might be an overestimation of compound mixing ratios in nitrogen-based GC effluent versus air-based online measurements.

## First measurements

We performed a series of test measurements to demonstrate the functionality and performance of the system. For all performed analyses we considered ions above  $m/z$  40, and ions detected at  $m/z$  31.018 ( $\text{CH}_3\text{O}^+$ ) and  $m/z$  33.033 ( $\text{CH}_3\text{O}^+$ ). In order to identify plant emissions and ozonolysis products we applied a Student's t-test<sup>29,30</sup> on the sets of data to be compared (e.g. mixing ratios in air entering the large plant chamber vs. mixing ratios in the large plant chamber; or mixing ratios in the reaction chamber with and without ozone, respectively). The Student's t-test returns a significance parameter,  $p$ , indicating the probability that the two datasets are not different. As threshold we used  $p=0.05$  indicating a 95% probability that the datasets are significantly different. The T-statistic parameter indicates the difference between the means of the two datasets (normalized by the variance) and was assigned separately for every type of experiment.

### Ozonolysis of $\beta$ -pinene

In order to test the functionality of the reaction chamber we performed an ozonolysis experiment with  $\beta$ -pinene, a reaction that has been widely studied.<sup>31-37</sup> During this experiment the flow through the reaction chamber was maintained at 7 L/min by two flow controllers which were set to 5 L/min and 2 L/min, respectively. This resulted in an air residence time of 11.5 minutes in the reaction chamber. The larger flow contained ~350 nmol/mol of  $\beta$ -pinene, which was produced by diluting a small flow (20 mL/min) of headspace air from a flask with liquid  $\beta$ -pinene (Sigma Aldrich, 99%) into the larger flow of purified air. Ozone levels of 1.3  $\mu\text{mol/mol}$  were produced in the 2 L/min flow by the ozone generator corresponding to ~370 nmol/mol ozone mixing ratio in the reaction chamber. Fig. 5 shows the course of  $\beta$ -pinene, some oxidation products, and the ozone mixing ratios. After ~one hour of adding ozone to the reaction chamber,  $\beta$ -pinene and ozone mixing ratios in the reaction chamber reached equilibrium: [ $\beta$ -pinene]~220 nmol/mol and [ $\text{O}_3$ ]~340 nmol/mol.

During  $\beta$ -pinene ozonolysis experiment analysis, we used 10 as threshold for the T-statistic parameter. Since reactions of ozone with contamination on the chamber walls were not constrained by a separate experiment, we applied additional filter by rejecting all species with a yield that was below 0.25%. As a result, among the oxidation products of  $\beta$ -pinene, we observed formaldehyde (detected as  $\text{CH}_3\text{O}^+$ ,  $m/z$  31.018), acetone (detected as  $\text{C}_3\text{H}_7\text{O}^+$ ,  $m/z$  59.049) and nopinone (detected as  $\text{C}_9\text{H}_{15}\text{O}^+$ ,  $m/z$  139.112 and fragmented as  $\text{C}_9\text{H}_{13}^+$ ,  $m/z$  121.102). The yields of all observed oxidation products are presented and compared to the yields from literature in Table 2. The comparison indicated that the yields obtained in this study are somewhat lower (except for acetone) than the yields described in literature. The lower yields were potentially caused by (i) the shorter residence time of air in the reaction chamber (11.5 minutes) in comparison with other studies<sup>31-37</sup>, (ii) lower  $\beta$ -pinene and ozone mixing ratios, and/or (iii) the absence of an OH scavenger<sup>38</sup> which would lead to a longer time for the system to reach equilibrium.

In addition to known compounds, several other compounds were observed, which had not been described previously. These newly observed compounds show the potential of the setup to identify more products of the oxidation of  $\beta$ -pinene, when improved cleaning protocols are followed and background measurements are performed. Finally, we observed that mixing ratios of sticky compounds like formic acid ( $m/z$  47.013) increased slower in the reaction chamber than other compounds (Fig. 5), indicating that a fraction of these products are lost to the walls of the reaction chamber. However, the loss is limited and towards the end of the experiment (~200 min, Fig. 5) the gas phase levels of  $m/z$  47.013 were in equilibrium.

### Birch seedling experiments

The first experiment (A) was performed on 4-5 August 2012, the second (B) – on 22-23 August 2012 and the third (C) – on 24-25 August 2012. Birch (*Betula pendula*) seedlings were collected with their surrounding sandy soil from a forest close to the Utrecht University campus 1-2 days before the experiments, and placed in 250 mL pots. The seedlings were 1-2 years old. In each experiment, the plant leaves in the large plant chambers had a total dry weight of 4.1-5.3 g, and a total leaf area of 1296-1413  $\text{cm}^2$ . Due to weather conditions, the soil of seedlings used in experiment C was very dry. After transfer to the lab, the seedlings were placed next to the large plant chambers, where the TL-D lamps produced light levels of 130-150  $\mu\text{mol}/\text{m}^2/\text{s}$  PAR with a light period from 7 am till 11 pm LT (16 h light, 8 h dark). Day and night temperatures in the large plant chambers were stable and equal to 25.7 $\pm$ 0.1 and 22.0 $\pm$ 0.1  $^\circ\text{C}$ , respectively. Relative humidity was 40-60%. Three plants were put into each large plant chamber. After the lids were closed the air flow of 2.5 L/min was maintained for 30 minutes before the start of the experiment to allow plant emissions to stabilize. Some water condensation was observed in the plant chambers several hours after the start of the experiments.

After the experiment, leaves were harvested, fresh weight was measured and leaf area was determined with a Li-3100 Area Meter (Lincoln, Nebraska, USA). Dry weight was measured after placing the leaves in an oven at 70  $^\circ\text{C}$  for at least 48 hours. Before experiments B and C, the reaction chamber was pre-cleaned overnight by flushing with purified air containing ozone mixing ratios of ~430 nmol/mol. To check if chambers were clean, background measurements (with purified air) of empty plant and reaction chambers were made. The

experiments were performed according to the measurement cycle described in section ‘Operation of the system’.

### Emission rates of birch seedlings

Emission rates (ER) of the birch seedlings were calculated according to equation 2:

$$ER = \frac{[\text{VOC}] * F_{\text{cham}}}{DW} \quad (2)$$

Where [VOC] is the mixing ratio (in nmol/mol, with subtracted background),  $F_{\text{cham}}$  is the air flow through the large plant chambers in mol/h, and DW is the leaf dry weight of the measured plants in g. The resulting emission rate has the unit of nmol/g(DW)/h. As a background we used the mixing ratios of species in the purified air supplied into the large plant chambers. All three experiments were used to calculate emission rates during the day (from the start of the experiment till 10 pm and from 9 am till the end of the experiment) and night (from 12 pm till 6 am).

During emission rates analysis as threshold for the T-statistic parameter we used 2.8. Consequently, a broad spectrum of the emitted compounds was observed indicating the good sensitivity of the system even towards the compounds emitted in low quantities during the day as well as during the night (Table 3). The observed monoterpene emission rates (0.69 nmol/g/h or 93.9 ng/g/h) were similar to rates reported by König et al.<sup>28</sup> (101.1 ng/g/h). However, they were significantly lower than some of the rates reported by Hakola et al.<sup>39</sup> (51-12469 ng/g/h) which could be explained by two factors. First, growth stage of plants strongly influences plant emission potentials and depends on a period of the year. Second, the lower light levels used in the current study would cause lower emissions.

The observed night time emissions for several species likely originate from the soil or pot, as *Betula pendula* leaf emissions have been shown to originate only from de novo production in response to light.<sup>40</sup> Covering pots with plants around the plant stem with Teflon film might exclude observed nocturnal emissions. The use of the small plant chambers (where no pots and roots are enclosed in the plant chamber) would exclude confounding emissions from the pot and/or soil in future experiments.

### Ozonolysis of birch emissions

Ozonolysis of the birch seedling emissions was performed by ozone additions into the reaction chamber (see section ‘Operation of the system’). Yields of the ozonolysis products were calculated according to equation 3:

$$yield = \frac{[\text{product}]_{\text{after}} - [\text{product}]_0}{[\text{monoterpenes}]_0 - [\text{monoterpenes}]_{\text{after}}} \quad (3)$$

Where [product]<sub>after</sub> and [product]<sub>0</sub> are the mixing ratios (in nmol/mol) of the product after and before the ozone addition, and [monoterpenes]<sub>after</sub> and [monoterpenes]<sub>0</sub> - the mixing ratios (in nmol/mol) of monoterpenes after and before ozone addition, respectively.

During further analysis we used 3 as threshold for the T-statistic parameter. As contamination of the chamber walls was an issue for these experiments, the following two additional criteria had to be satisfied (further called ‘filters’): a) the night time yield had to be smaller than the yield during the following day; b) the change in the mixing ratio upon ozonolysis had to be above 27 pmol/mol (which corresponds to the detection limit of PTR-TOF-MS).

Fig. 6 shows the course of the measured ozone and monoterpene mixing ratios. Minimum monoterpene mixing ratios and maximum ozone mixing ratios were observed at the same time in the reaction chamber demonstrating that chemical reactions with ozone were the cause of monoterpenes depletion.<sup>41</sup> We modeled the monoterpene mixing ratios in the reaction chamber during the period shown in Fig. 6 in order to check if the degradation rate of monoterpenes was in agreement with the measured ozonolysis rate constants of the observed monoterpenes emitted from the birch seedlings. The initial monoterpenes mixing ratio, the mixing ratio of ozone, and first order kinetics were used. The initial monoterpenes mixing ratio was attributed to individual monoterpenes by using the information from the chromatogram shown in Fig. 4D. The relative fractions were 0.28, 0.47, and 0.25 for  $\alpha$ -pinene, d-limonene, and  $\beta$ -phellandrene, respectively. The reaction rates for these compounds with ozone have been measured to be  $8.7 \times 10^{-17}$ ,  $2.0 \times 10^{-16}$  and  $4.8 \times 10^{-17}$   $\text{cm}^3 \text{molec}^{-1} \text{s}^{-1}$ , respectively.<sup>42-43</sup> Using this information the degradation of the monoterpenes was calculated separately and the total monoterpene mixing ratio at every time step was calculated as the sum of the individual contributions. The measured and modeled monoterpene mixing ratios (see Fig. 6) agree reasonably well, showing that the general description of the observed chemistry in the reaction chamber is adequate. Somewhat lower measured monoterpene mixing ratios in comparison to the calculated values were associated with the absence of an OH scavenger<sup>38</sup> in the system which could lead to a faster monoterpene degradation due to reactions with the OH radical.

Fig. 7 shows averaged monoterpene mixing ratios measured online in the reaction chamber before and after ozone addition in experiment B. The decrease of monoterpene signal during/after ozonolysis as shown in Fig. 6 and described above was well reproducible. Due to the low primary signal the sensitivity of the instrument during experiment B was rather low which caused the detection of only few ions produced during the ozonolysis. Despite the reasonable understanding of the chemistry happening in the reaction chamber it was difficult to identify ozonolysis products from experiments A-C. The reaction chamber was not well cleaned before the start of experiment A and ozonolysis products were also from contamination, i.e. reactive organic species sticking to the walls of the reaction chamber system. For example, during experiment A the production of  $m/z$  61.029 (calculated as a difference in mixing ratios for an ion in the reaction chamber with and without ozone added) during the night was higher than during the following day, despite much lower monoterpene levels during the night. This indicated a significant contribution from contamination to the signal of the ion, and in experiment A a similar behavior was observed for many other ions. In the experiments B and C the proper cleaning procedure was applied, therefore the above mentioned problems were not encountered. The change in monoterpenes mixing ratio upon the ozone addition was below the detection limit of PTR-TOF-MS due to very low plant emissions in experiment C. Therefore, it was not possible to calculate the yields for experiment C and apply the filter (a).

In order to overcome these issues the above mentioned filters were developed. Initially we detected 193 ions during experiments A, B and C. Of these, 43 and 60 ions passed the Student's t-test in experiment A and B, respectively. None of the 43 ions from experiment A and only 2 ions from the 60 ions from experiment B passed the additional filters (a) and (b):  $m/z$

47.048 (corresponding to the molecular formula  $\text{C}_2\text{H}_7\text{O}^+$ ) with a molar yield  $25.9 \pm 9.8\%$  and  $m/z$  73.029 (corresponding to the molecular formula  $\text{C}_3\text{H}_5\text{O}_2^+$ ) with a molar yield  $29.5 \pm 8.2\%$ .

Despite the low number of detected ozonolysis products, the above mentioned experiments demonstrated the capability of the system to detect ozonolysis products even at low mixing ratios of the parent compounds which can be improved by better reaction chamber pre-cleaning protocols and better (standard) PTR-TOF-MS performance, in which case the number of ions removed by filters (a) and (b) would be much reduced.

#### Arabidopsis experiments

*Arabidopsis thaliana* Col-0 plants were stratified (dark, 4 °C, 3 days) and subsequently grown in soil (8 h light, 16 h dark, 160  $\mu\text{mol m}^{-2} \text{s}^{-1}$  PAR,  $20 \pm 2$  °C, 70% RH). After 10 days, seedlings were transferred to individual 70 mL pots. Four-week old plants were transferred to the plant chamber setup (same light period) and allowed to acclimatize before they were placed into the small plant chambers. The UV-B lamp was turned on from 10 am till 2 pm LT at an intensity of 0.1  $\text{W m}^{-2}$ , so that the plant in small plant chamber #2 (with quartz lid) was exposed to UV-B light for four hours, while the plant in #1 (with glass lid) was not. We observed higher emissions of *Arabidopsis* plants upon UV-B exposure for several compounds. Fig. 8 shows the average emission of  $m/z$  61.029 during the 4-hour UV-B exposure period in three individual experiments, as an example. This shows that changes in BVOC emissions upon UV-B exposure can be induced for the genetic model plant species *Arabidopsis thaliana*.

#### Conclusions

The setup to measure impact of pollution on plant emissions was tested and first results are shown to demonstrate the performance. In the  $\beta$ -pinene ozonolysis experiment the expected products were observed, although with somewhat lower yields than described in the literature. In the experiments with real plant emissions, mixing ratios in the large plant chambers and the reaction chamber were shown to generally coincide, showing good quantitative transfer of the VOCs between these components of the setup.

The sampling efficiency of the GC system has been tested. The recovery factors were within the range of 0.71 - 1.38, indicating that cryogenic sampling and the transfer through the GC system is adequate. The added value of the GC part of the system was clear from the analysis of birch seedling emissions, where it allowed us to distinguish three specific monoterpenes within the birch monoterpene emissions.

We performed experiments with birch seedlings and found emission of 14 species. The observed day time emission rates are in agreement with rates observed by König et al.<sup>28</sup> and are lower than some rates observed by Hakola et al.<sup>39</sup> The latter is likely caused by the difference in growth stage of the used plants and the fact that latter measurements were performed in the field, thus with higher light intensities. Addition of ozone to the birch seedling emissions resulted in decreased monoterpene mixing ratios. The modeled monoterpene mixing ratios in the reaction chamber agreed reasonably well with the measured levels. Our results show that our setup is capable of detecting ozonolysis products at low levels (<1 nmol/mol) of biogenic emissions, although few ozonolysis products were observed. The experiments performed with *Arabidopsis thaliana* plants

using the small plant chambers and UV-B lamp show that our setup can also be used to study volatile emission responses upon UV-B, even in small plants like *Arabidopsis*. This opens up a range of possibilities to study the biological mechanisms underpinning plant volatile emissions, since there is a vast array of mutants and genetic information available on this important plant model species. The operation of the setup thus is flexible and the use of optional plant chambers allows for a broad spectrum of experiments. E.g., the discrepancy between the observed and predicted chemical loss of ozone via reactions with plant emissions, the impact of pollution on plant emissions can be studied. The full automatization of the system allows easy-to-perform long- and short-term measurements.

Further improvements and enhancements of the experimental setup include: a) attaching leaf thermocouples to plant leaves and including fans in the chambers; b) increasing light intensity in the plant chambers through for example LEDs, which cause lower heating than conventional lamps, to obtain plant VOC emissions that are more similar to those under natural conditions; c) installing a system to control OH and NO<sub>x</sub> mixing ratios in the reaction chamber, so that ozonolysis under NO<sub>x</sub>/VOC limiting conditions can be studied; and d) adding UV light to the reaction chamber, so that ozone yield from photochemical ozone production from plant emissions can be measured.

### Acknowledgements

The TD-PTR-MS has been funded by the Netherlands Organization for Scientific Research (NWO) under the ALW-Middelgroot program (Grant 834.08.002). This project is funded by a strategic funding scheme (Focus and Mass) of Utrecht University. We would like to thank Carina van der Veen, Henk Snellen, Michel Bolder and Marcel Portanger of Utrecht University, the Netherlands for the excellent technical support and L.A.C.J. Voeselek and Thomas Röckmann for scientific discussion.

### Notes and references

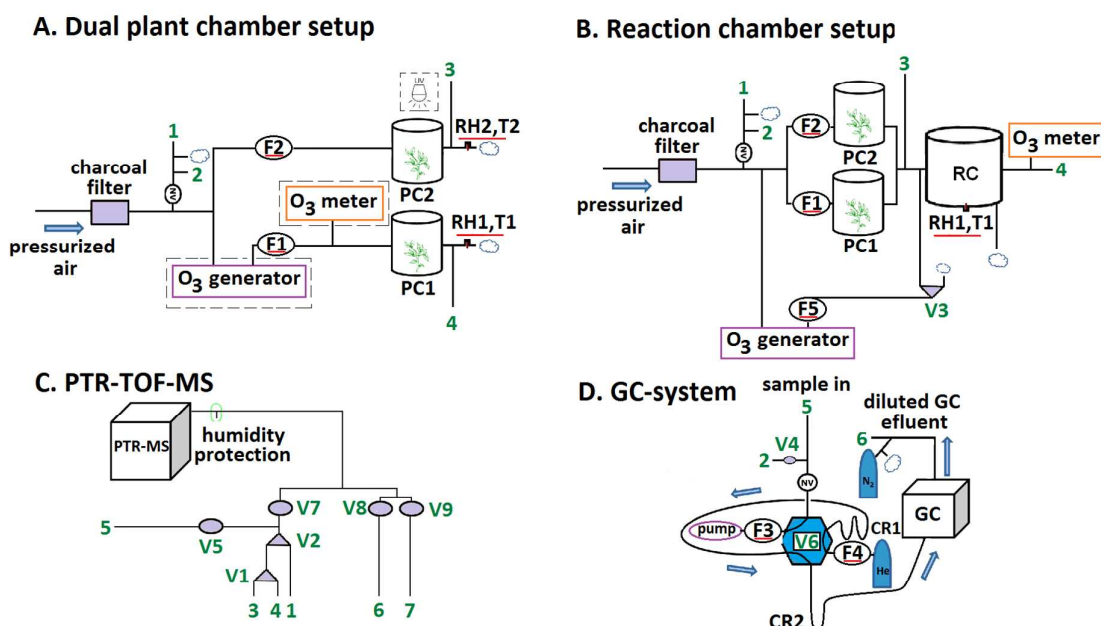
<sup>a</sup> Institute for Marine and Atmospheric Research Utrecht, Utrecht University, The Netherlands.

<sup>b</sup> Plant Ecophysiology, Institute of Environmental Biology, Utrecht University, the Netherlands.

- F. Fehsenfeld, J. Calvert, R. Fall, P. Goldan, A. B. Guenther, C. N. Hewitt, B. Lamb, S. Liu, M. Trainer, H. Westberg and P. Zimmerman: Emissions of volatile organic compounds from vegetation and the implications for atmospheric chemistry, *Global Biogeochem. Cy.*, 1992, **6(4)**, 389–430.
- I. Riipinen, J. R. Pierce, T. Yli-Juuti, T. Nieminen, S. Häkkinen, M. Ehn, H. Junninen, K. Lehtipalo, T. Petaja, J. Slowik, R. Chang, N.C. Shantz, J. Abbatt, W. R. Leaitch, V.-M. Kerminen, D. R. Worsnop, S. N. Pandis, N. M. Donahue and M. Kulmala: Organic condensation: a vital link connecting aerosol formation to cloud condensation nuclei (CCN) concentrations, *Atmos. Chem. Phys.*, 2011, **11(8)**, 3865–3878.
- L. K. Sahu: Volatile organic compounds and their measurements in the troposphere, *Curr. Sci. India*, 2012, **102(12)**, 1645–1649.
- A. Guenther, T. Karl, P. Harley, C. Wiedinmyer, P.I. Palmer and C. Geron: Estimates of global terrestrial isoprene emissions using MEGAN (Model of Emissions of Gases and Aerosols from Nature), *Atmos. Chem. Phys.*, 2006, **6**, 3181–3210.
- K. L. Denman, G. Brasseur, A. Chidthaisong, P. Ciais, P. M. Cox, R. E. Dickinson, D. Hauglustaine, C. Heinze, E. Holland, D. Jacob, U. Lohmann, S. Ramachandran, P. L. da Silva Dias, S. C. Wofsy, and X. Zhang: *Climate Change 2007: The Physical Science Basis. Contribution of Working Group I to the Fourth Assessment Report of the Intergovernmental Panel on Climate Change*; New York: Cambridge University Press, 2007.
- S.T. Summerfelt and J.N. Hochheimer: Review of ozone processes and applications as an oxidizing agent in aquaculture, *Prog. Fish-Cult.*, 1997, **59**, 94–105.
- A. H. Goldstein and I. E. Galbally: Known and unexplored organic constituents in the Earth's Atmosphere, *Environ. Sci. Technol.*, 2007, **41**, 1514–1521.
- M. Kulmala: How particles nucleate and grow, *Science*, 2003, **302**, 1000–1001.
- R. M. Harrison, and J. Yin: Particulate matter in the atmosphere: which particle properties are important for its effects on health? *Sci. Total Environ.*, 2000, **249**, 85–101.
- M. O. Andreae, and P. J. Crutzen: Atmospheric Aerosols: Biogeochemical Sources and Role in Atmospheric Chemistry, *Science*, 1997, **276(2)**, 1052–1058.
- J. Beauchamp, A. Wisthaler, A. Hansel, E. Kleist and M. Miebach: Ozone induced emissions of biogenic VOC from tobacco: relationships between ozone uptake and emission of LOX products Volatile organic compound (VOC) emissions from tobacco, *Plant Cell Environ.*, 2005, **28**, 1334–1343.
- K. Hartikainen, J. Riikonen, A. Nerg, M. Kivimäenpää, V. Ahonen, A. Tervahauta, S. Kärenlampi, M. Mäenpää, M. Rousi, S. Kontunen-Soppela, E. Oksanen and T. Holopainen: Impact of elevated temperature and ozone on the emission of volatile organic compounds and gas exchange of silver birch (*Betula pendula* Roth), *Environ. Exp. Bot.*, 2012, **84**, 33–43.
- T. Karl, P. Harley, L. Emmons, B. Thornton, A. Guenther, C. Basu, A. Turnipseed and K. Jardine: Efficient atmospheric cleansing of oxidized organic trace gases by vegetation, *Science*, 2010, **330(6005)**, 816–819.
- Ü. Niinemets: Mild versus severe stress and BVOCs: thresholds, priming and consequences, *Trends Plant Sci.*, 2009, **15(3)**, 145–153.
- A. Guenther, C. Geron, T. Pierce, B. Lamb, P. Harley and R. Fall: Natural emissions of non-methane volatile organic compounds, carbon monoxide, and oxides of nitrogen from North America, *Atmos. Environ.*, 2000, **34**, 2205–2230.
- W. Kegge, and R. Pierik: Biogenic volatile organic compounds and plant competition, *Trends Plant Sci.*, 2009, **15(3)**, 126–132.
- W. Kegge, B.T. Weldegergis, R. Soler, M. Vergeer-Van Eijk, M. Dicke, L.A.C.J. Voeselek, R. Pierik: Canopy light cues affect emission of constitutive and methyl jasmonate-induced volatile organic compounds in *Arabidopsis thaliana*, *New Phyt.*, 2013, **200(3)**, 861–874.
- T. F. Mentel, J. Wildt, A. Kiendler-Scharr, E. Kleist, R. Tillmann, M. Dal Maso, R. Fisseha, Th. Hohaus, H. Spahn, R. Uerlings, R. Wegener, P.T. Griffiths, E. Dinar, Y. Rudich, and A. Wahner: Photochemical production of aerosols from real plant emissions. *Atmos. Chem. Phys.*, 2009, **9**, 4387–4406.
- T. Karl, P. Harley, A. Guenther, R. Rasmussen, B. Baker, K. Jardine, and E. Nemitz: The bi-directional exchange of oxygenated VOCs

- between a loblolly pine (*Pinus taeda*) plantation and the atmosphere, *Atmos. Chem. Phys.*, 2005, **5**, 3015–3031.
- 20 A. Jordan, S. Haidacher, G. Hanel, E. Hartungen, L. Märk, H. Seehauser, R. Schottkowsky, P. Sulzer and T.D. Mark: A high resolution and high sensitivity proton-transfer-reaction time-of-flight mass spectrometer (PTR-TOF-MS), *Int. J. Mass Spectrom.*, 2009, **286(2-3)**, 122–128.
- 21 M. Graus, M. Muller, and A. Hansel: High Resolution PTRTOF: Quantification and Formula Confirmation of VOC in Real Time, *J. Am. Soc. Mass Spectr.*, 2010, **21**, 1037–1044.
- 22 V. Falara, T. A. Akhtar, T. T. H. Nguyen, E. A. Spyropoulou, P. M. Bleeker, I. Schauvinhold, Y. Matsuba, M.E. Bonini, A.L. Schillmiller, R.L. Last, R.C. Schuurink and E. Pichersky: The tomato terpene synthase gene family, *Plant Physiol.*, 2011, **157**, 770–789.
- 23 M. A. Ibrahim, M. Mäenpää, V. Hassinen, S. Kontunen-Soppela, L. Malec, M. Rousi, L. Pietikäinen, A. Tervahauta, S. Kärenlampi, J.K. Holopainen and E.J. Oksanen: Elevation of night-time temperature increases terpenoid emissions from *Betula pendula* and *Populus tremula*, *J. Exp. Bot.*, 2010, **61(6)**, 1583–1595.
- 24 R.M.P. van Poecke, M. A. Posthumus and M. Dicke: Herbivore-induced volatile production by *Arabidopsis thaliana* leads to attraction of the parasitoid *Cotesia rubecula*: chemical, behavioral, and gene-expression analysis, *J. Chem. Ecol.*, 2001, **27(10)**, 1911–1928.
- 25 R. Holzinger, A. Kasper-Giebl, M. Staudinger, G. Schauer and T. Röckmann: Analysis of the chemical composition of organic aerosol at the Mt. Sonnblick observatory using a novel high mass resolution thermal-desorption proton-transfer-reaction mass-spectrometer (hr-TD-PTR-MS), *Atmos. Chem. Phys.*, 2010, **10**, 10111–10128.
- 26 R. Holzinger, J. Williams, F. Herrmann, J. Lelieveld, N. M. Donahue and T. Röckmann: Aerosol analysis using a Thermal-Desorption Proton-Transfer-Reaction Mass Spectrometer (TD-PTR-MS): a new approach to study processing of organic aerosols, *Atmos. Chem. Phys.*, 2010, **10**, 2257–2267.
- 27 K.L. Goodner: Practical retention index models of OV-101, DB-1, DB-5, and DB-Wax for flavor and fragrance compounds, *Food Sci. Technol.*, 2008, **41**, 951–958.
- 28 G. König, M. Brunda, H. Puxbaum, C. N. Hewitt, S. C. Duckham and J. Rudolph: Relative contribution of oxygenated hydrocarbons to the total biogenic VOC emissions of selected mid-European agricultural and natural plant species, *Atmos. Environ.*, 1995, **29(8)**, 861–874.
- 29 D.C. Leblanc: Statistics - Concepts and Applications for Science, 189, Jones and Bartlett, Sudbury, MA, 2004.
- 30 I.B. Weiner and W.E. Craighead: Corsini Encyclopedia of Psychology, 1723, Hoboken, NJ, Wiley, 2010.
- 31 Arey, J., Atkinson R. and Aschmann, S. M.: Product study of the gas-phase reactions of monoterpenes with the OH radical in the presence of NO<sub>x</sub>, *J. Geophys. Res.*, 1990, **95(D11)**, 18539–18546.
- 32 S. Hatakeyama, K. Izumi and H. Akimoto: Reactions of OH with  $\alpha$ -pinene and  $\beta$ -pinene in air: estimate of global CO production from the atmospheric oxidation of terpenes, *J. Geophys. Res.*, 1991, **96(D1)**, 947–958.
- 33 J.J. Orlando, B. Noziere, G.S. Tyndall, G.E. Orzechowska, S.E. Paulson and Y. Rudich: Product studies of the OH- and ozone-initiated oxidation of some monoterpenes, *J. Geophys. Res.*, 2000, **105(D9)**, 11561–11572.
- 34 Bo.R. Larsen, D. Di Bella, M. Glasius, R. Winterhalter, N. R. Jensen and J. Hjorth: Gas-Phase OH Oxidation of Monoterpenes: Gaseous and Particulate Products, *J. Atmos. Chem.*, 2001, **38**, 231–276.
- 35 A. Wisthaler, N.R. Jensen, R. Winterhalter, W. Lindinger and J. Hjorth: Measurements of acetone and other gas phase product yields from the OH-initiated oxidation of terpenes by proton-transfer-reaction mass spectrometry (PTR-MS), *Atmos. Environ.*, 2001, **35**, 6181–6191.
- 36 M. Jaoui, and R. M. Kamens.: Mass balance of gaseous and particulate products from beta-pinene/O<sub>3</sub>/air in the absence of light and beta-pinene/NO<sub>x</sub>/air in the presence of natural sunlight, *J. Atmos. Chem.*, 2003, **45(2)**, 101–141.
- 37 A. Lee, A. H. Goldstein, J. H. Kroll, N. L. Ng, V. Varutbangkul, R. C. Flagan and J. H. Seinfeld: Gas-phase products and secondary aerosol yields from the photooxidation of 16 different terpenes, *J. Geophys. Res.*, 2006, **111**, D17305.
- 38 S.M. Aschmann, J. Arey and R. Atkinson: OH radical formation from the gas-phase reactions of O<sub>3</sub> with a series of terpenes, *Atmos. Environ.*, 2002, **36**, 4347–4355.
- 39 H. Hakola, J. Rinne and T. Laurila: The hydrocarbon emission rates of tea-leaved willow (*Salix Phyllicifolia*), silver birch (*Betula Pendula*) and European aspen (*Populus Tremula*), *Atmos. Environ.*, 1998, **32(10)**, 1825–1833.
- 40 A. Ghirardo, K. Koch, R. Taipale, I. Zimmer, J. P. Schnitzler, J. Rinne: Determination of de novo and pool emissions of terpenes from four common boreal/alpine trees by <sup>13</sup>C<sub>2</sub>O<sub>2</sub> labelling and PTR-MS analysis, *Plant Cell Environ.*, 2010, **33**, 781–792.
- 41 R. Atkinson and J. Arey: Gas-phase tropospheric chemistry of biogenic volatile organic compounds: a review, *Atmos. Environ.*, 2003, **37(2)**, 197–219.
- 42 B. Shorees, R. Atkinson and J. Arey: Product formation from the gas-phase reactions of OH radicals and O<sub>3</sub> with  $\beta$ -Phellandrene, *Int. J. Chem. Kinet.*, 1991, **23**, 897–906.
- 43 R. Atkinson: Gas-phase tropospheric chemistry of volatile organic compounds: 1. Alkanes and alkenes, *J. Phys. Chem. Ref. Data*, 1997, **26**, 215–290.

1

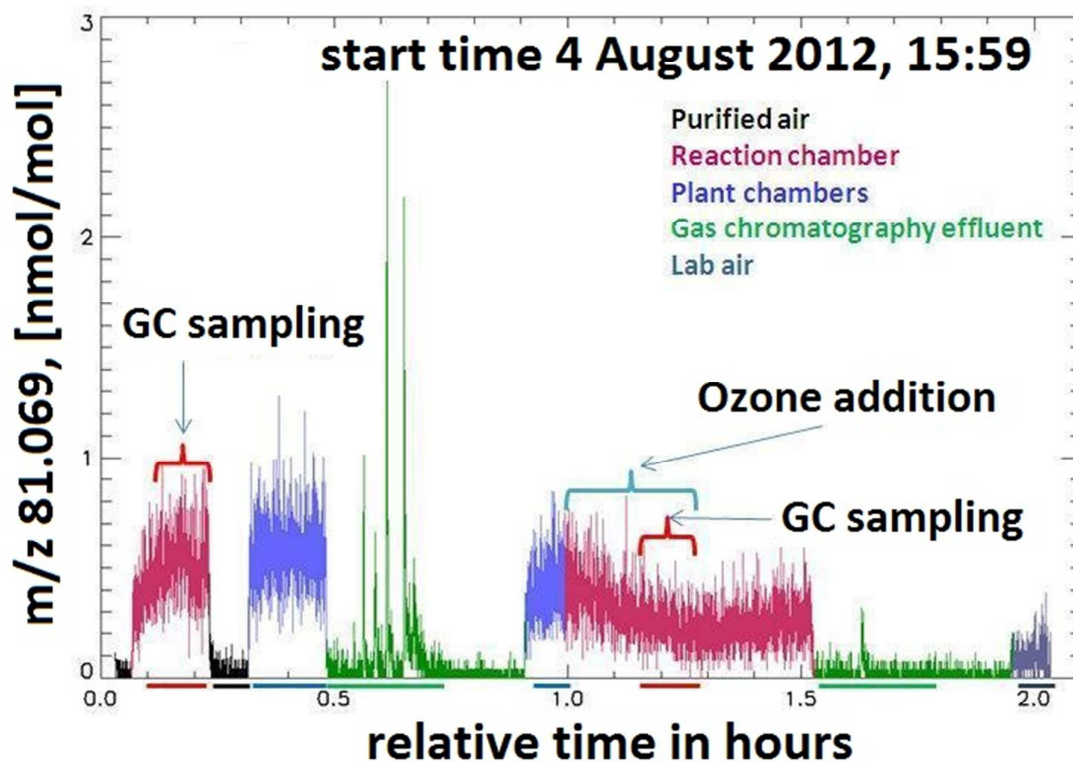


2

3 Fig. 1. Schematic overview of the setup with two optional chamber configurations (A and B),  
 4 PTR-TOF-MS connections (C) and GC sampling system (D). The parts of the system inside  
 5 dashed line boxes are optional (A). Port numbers 1, 3 and 4 indicate the sampling positions  
 6 for the PTR-TOF-MS. The GC samples through port 5 and the GC-effluent is analyzed with  
 7 the PTR-TOF-MS through port 6. Lab air is analyzed through port 7 and port 2 connects the  
 8 GC system to purified air for cleaning. The following abbreviations were used: NV – needle  
 9 valve, PC1, PC2 – large plant chambers; RC – reaction chamber, GC – gas chromatograph;  
 10 V1-V5 and V7-V9 – 2-way (circles) and 3-way (triangles) valves, V6 is a 6-port Valco valve;  
 11 F1,F2,F3,F4 – flow controllers; RH1, RH2, T1, T2 – temperature and relative humidity  
 12 sensors; CR1, CR2 – sampling and focusing cryotrap; N<sub>2</sub>, He – nitrogen and helium  
 13 cylinders; small clouds depict overflow outlets. The parameters which are underlined in red  
 14 are recorded during measurements. The little ‘clouds’ indicate overflow.

15

1

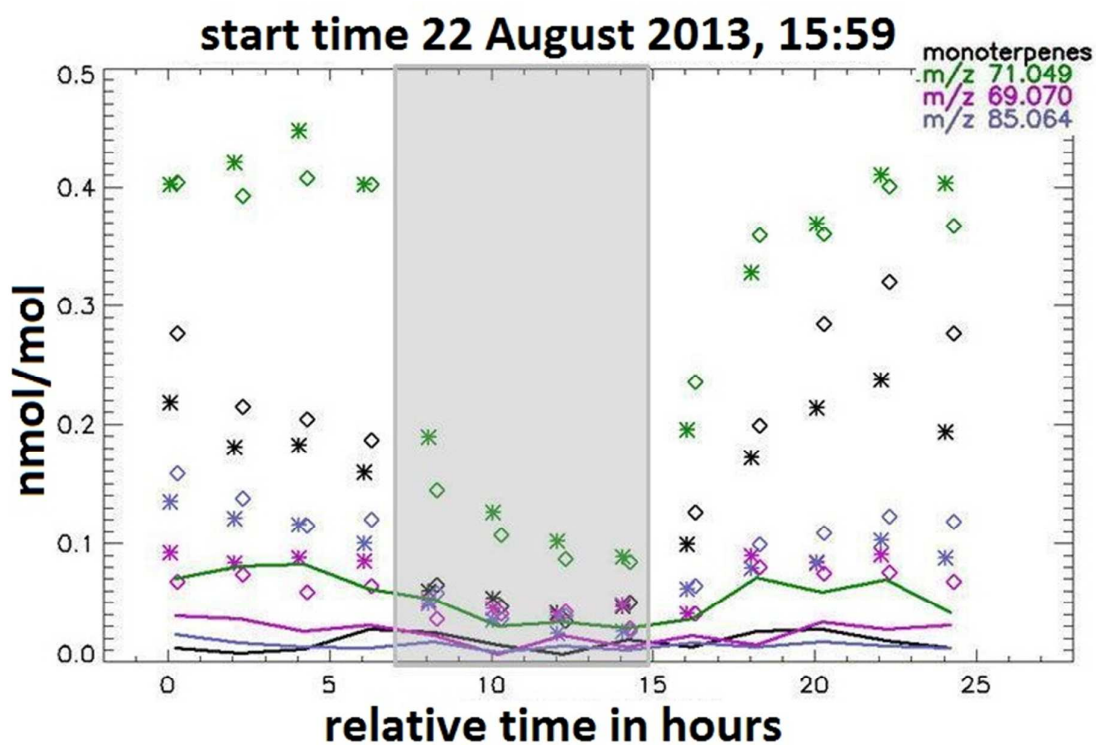


16

17

18 Fig. 2. The standard two-hour cycle of measurements. The signal observed at  $m/z$  81.069 is  
 19 shown as an example, and the color indicates what is measured at a given moment (see  
 20 legend). The brackets in the plot area indicate GC sampling and ozone addition periods.  
 21 Colored lines under the x-axis depict the averaging/integration period for averaged/integrated  
 22 data as used in Fig. 3 and 7: last 7 minutes of first reaction chamber air, last 4 minutes of  
 23 purified air, last 9 minutes of large plant chamber air, last 9 minutes of second large plant  
 24 chamber air, last 7 minutes of second reaction chamber air (ozone treatment).

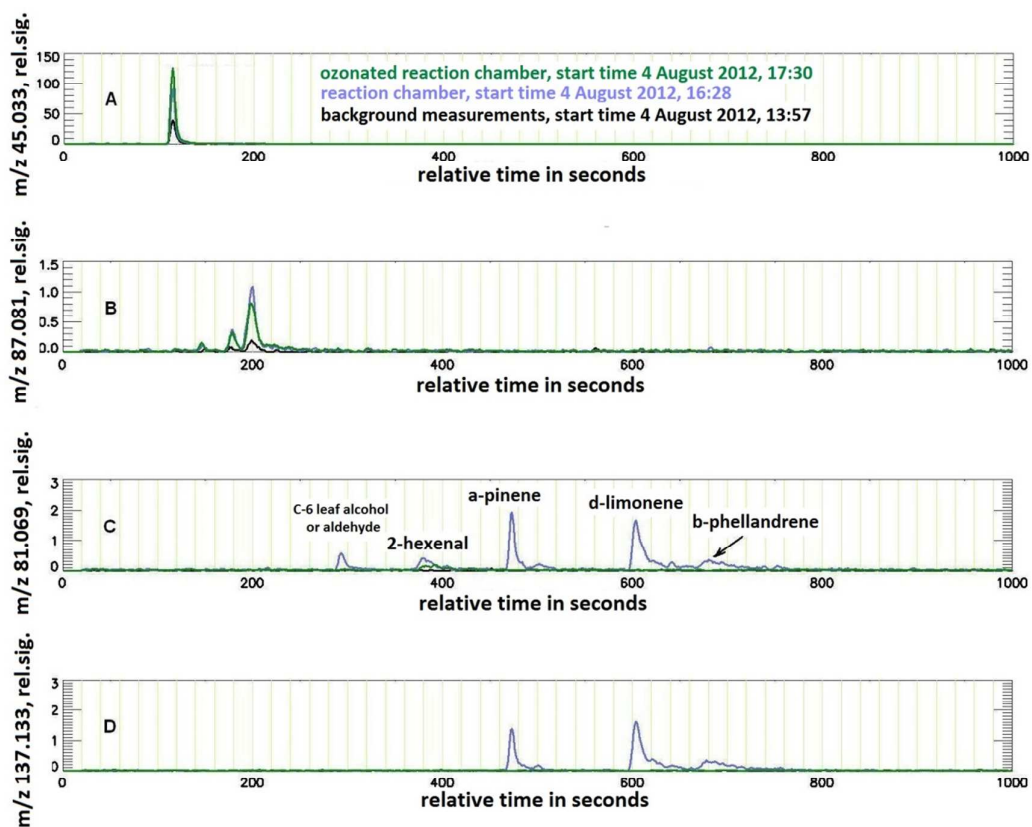
25



26

27 Fig. 3. Online measured mixing ratios in the large plant chambers (diamonds) and in the  
28 reaction chamber without ozone addition (asterisks), experiment B. The respective  
29 background levels (purified air) are shown as continuous lines. The shaded area indicates the  
30 dark period.

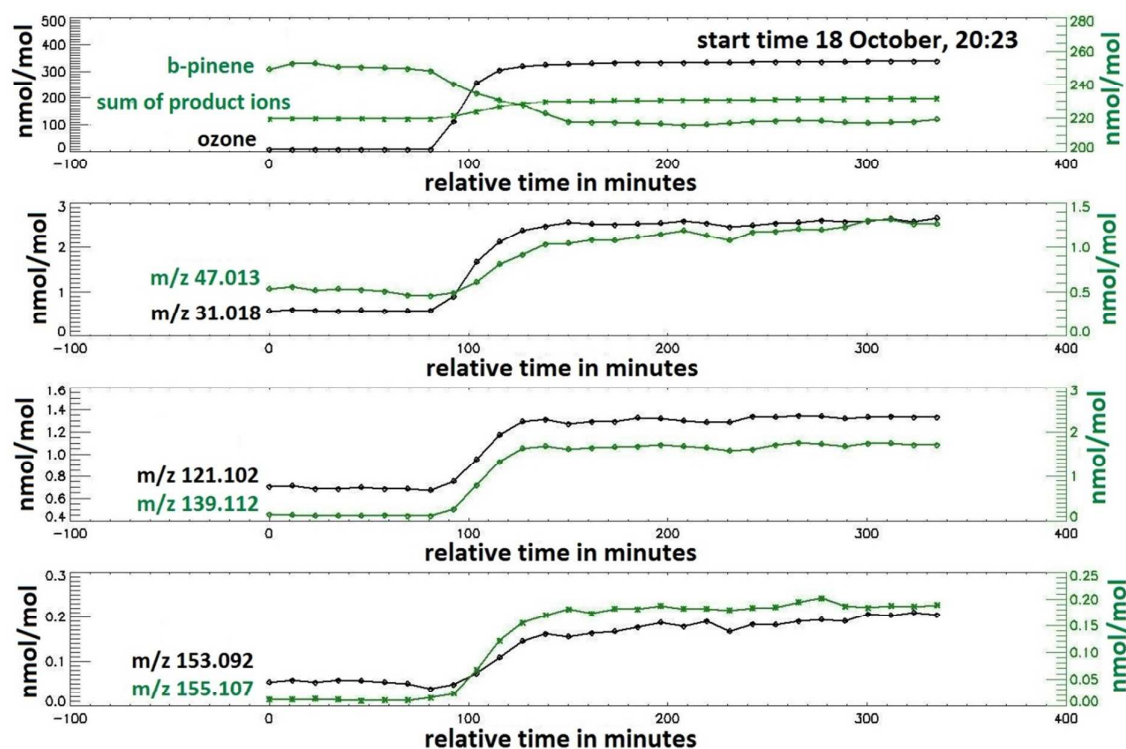
31



32

33 Fig. 4. Example gas chromatograms of experiment A. For every profile running mean over 5  
 34 points is used. The green line and the blue line correspond to sampling the ozonated and non-  
 35 ozonated reaction chamber, respectively. The black line is a background chromatogram. M/z  
 36 45.033 corresponds to acetaldehyde, m/z 87.081 to methyl buthenol (MBO), m/z 81.069 to  
 37 monoterpenes and additional compounds, m/z 137.133 to monoterpenes only.

38

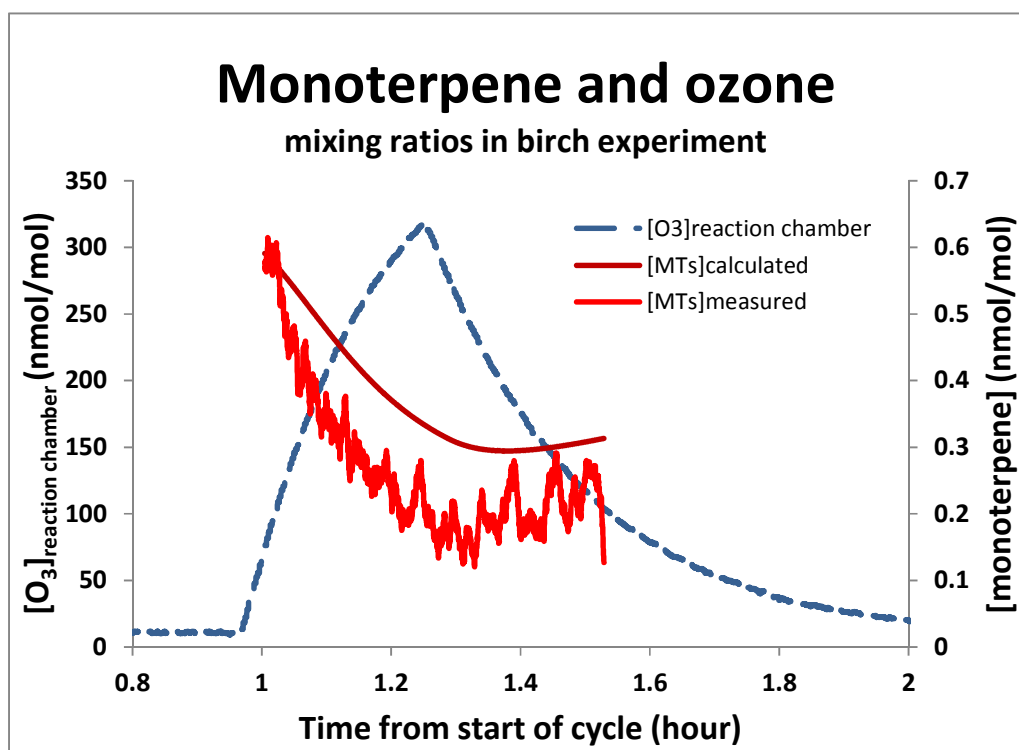


39

40

41 Fig. 5. Ozonolysis of  $\beta$ -pinene. The top panel shows the course of ozone,  $\beta$ -pinene (sum of  
42  $m/z$  81.069 and 137.133) and the sum of all product ions (note that an offset of 210 nmol/mol  
43 has been added). The lower panels show oxidation products detected at  $m/z$  31.018  
44 (formaldehyde), 47.013 (formic acid), 121.102 and 139.112 (attributed to nopinone), 153.092  
45 ( $C_9H_{13}O_2^+$ ), and 155.107 ( $C_9H_{15}O_2^+$ ). Ozone was added to the reaction chamber 85 minutes  
46 after the start of the measurements. Presented points are averaged mixing ratios of 11.5  
47 minutes time periods, which corresponds to the residence time of the air in the reaction  
48 chamber.

49

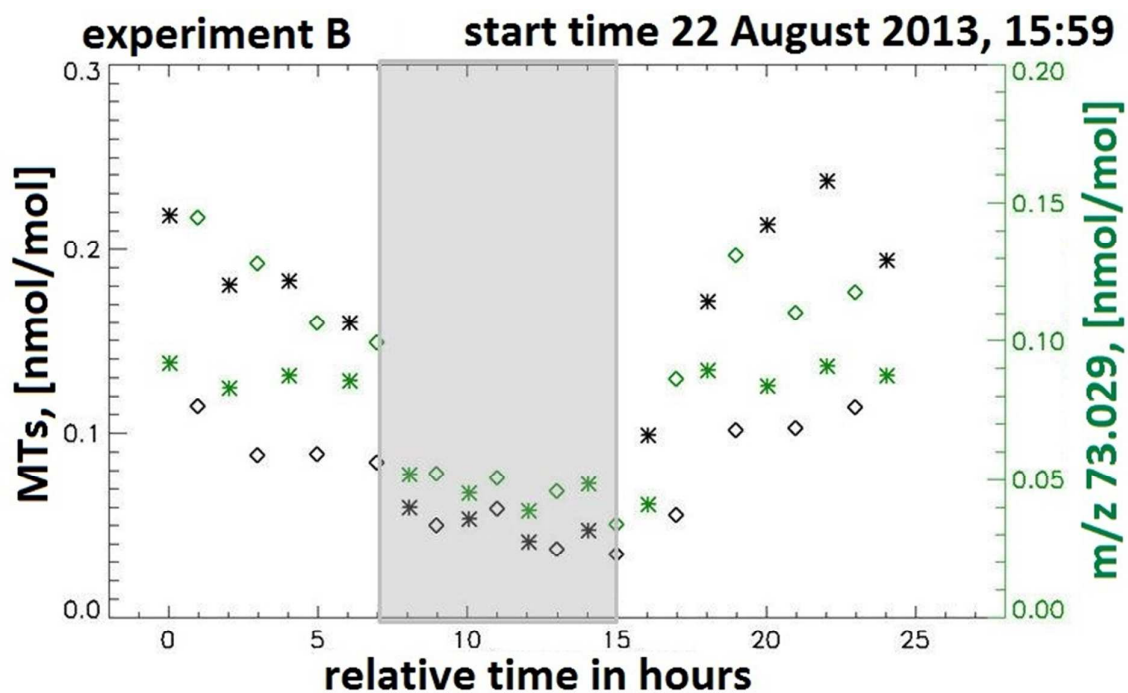


50

51

52 Fig. 6. Measured and modeled monoterpene and ozone profiles.  $[O_3]_{\text{reaction chamber}}$  is the ozone  
53 mixing ratios in the reaction chamber.  $[MTs]_{\text{measured}}$  corresponds to the monoterpene mixing  
54 ratios in the reaction chamber;  $[MTs]_{\text{calculated}}$  corresponds to the monoterpene mixing ratios in  
55 the reaction chamber calculated as described in section 3.3. Presented measured monoterpene  
56 data are averaged over 2 minutes.

57

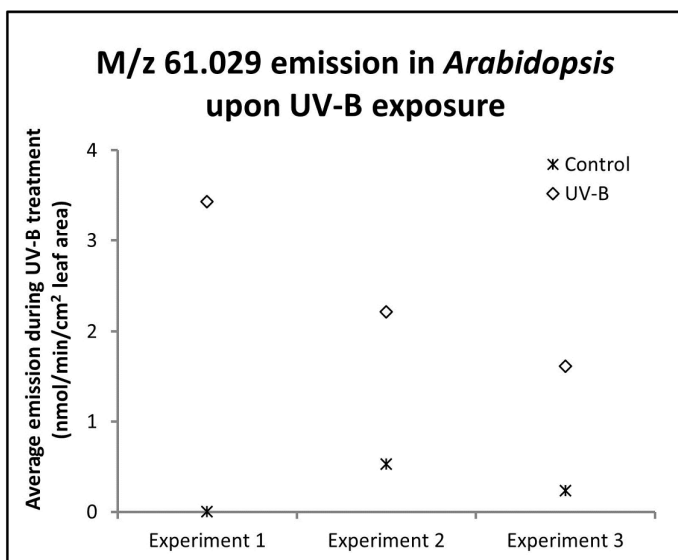


58

59

60 Fig. 7. Online measured mixing ratios of monoterpenes (MTs) and m/z 73.029 in the reaction  
61 chamber without ozone addition (asterisks) and during/after ozone addition (diamonds),  
62 experiment B. The shaded area indicates the dark period.

63



64

65 Fig. 8. *Arabidopsis thaliana* emissions of m/z 61.029 during a 4-hour UV-B exposure period  
66 in exposed and control plants. Four-week old plants of the ecotype Col-0 were used. Over the  
67 three individual experiment shown, average emissions of UV-treated plants were significantly  
68 higher than emissions of control plants (Student's t-test,  $p=0.047$ ).

69

70

71 Table 1. Recovery factors (RF) for several compounds, calculated from experiment A, B and  
72 C using equation 3. All chromatograms that sampled from the ozone free reaction chamber  
73 have been included into this analysis (n=40). Numbers shown are averages  $\pm$  SD.

Compound or m/z	Formula•H <sup>+</sup>	RF $\pm$ SD
33.033	CH <sub>4</sub> OH <sup>+</sup>	0.75 $\pm$ 0.10
43.018	C <sub>2</sub> H <sub>3</sub> O <sup>+</sup>	0.82 $\pm$ 0.07
59.049	C <sub>3</sub> H <sub>7</sub> O <sup>+</sup>	0.71 $\pm$ 0.08
61.029	C <sub>2</sub> H <sub>5</sub> O <sub>2</sub> <sup>+</sup>	1.38 $\pm$ 0.26
69.07	C <sub>5</sub> H <sub>9</sub> <sup>+</sup>	1.09 $\pm$ 0.28
87.045	C <sub>4</sub> H <sub>7</sub> O <sub>2</sub> <sup>+</sup>	1.10 $\pm$ 0.16
87.081	C <sub>5</sub> H <sub>11</sub> O <sup>+</sup>	1.20 $\pm$ 0.25
monoterpenes	C <sub>10</sub> H <sub>17</sub> <sup>+</sup>	1.23 $\pm$ 0.31

74

75

76 Table 2. Molar yields of ozonolysis products of  $\beta$ -pinene obtained in this study and in the  
 77 literature (Lee et al., 2006<sup>a</sup>; Arey et al., 1990<sup>b</sup>; Hatakeyama et al., 1991<sup>c</sup>; Jaoui and Kamens,  
 78 2003<sup>d</sup>; Larsen et al., 2001<sup>e</sup>; Orlando et al., 2000<sup>f</sup>; Wisthaler et al., 2001<sup>g</sup>).

Product	m/z	Formula•H <sup>+</sup>	Yield, % [literature]	Yield, % [this work]
formaldehyde	31.018	CH <sub>3</sub> O <sup>+</sup>	23 <sup>e</sup> -54 <sup>c</sup>	5.9
	33.033	CH <sub>4</sub> OH <sup>+</sup>		0.35
	41.038	C <sub>3</sub> H <sub>5</sub> <sup>+</sup>		0.53
	43.018	C <sub>2</sub> H <sub>3</sub> O <sup>+</sup>		4.17
acetaldehyde	45.033	C <sub>2</sub> H <sub>4</sub> O	0.6 <sup>a</sup>	1.07
formic acid	47.013	HCOOH <sub>2</sub> <sup>+</sup>	2.0 <sup>f</sup> -38.0 <sup>e</sup>	1.76
	47.022	no match		0.42
acetone	59.049	C <sub>3</sub> H <sub>7</sub> O <sup>+</sup>	2.0 <sup>f</sup> -16.0 <sup>g</sup>	16.90
acetic acid	61.029	C <sub>2</sub> H <sub>5</sub> O <sub>2</sub> <sup>+</sup>	1.4 <sup>a</sup>	0.98
	73.029	C <sub>3</sub> H <sub>5</sub> O <sub>2</sub> <sup>+</sup>		0.28
	83.050	C <sub>5</sub> H <sub>7</sub> O <sup>+</sup>		1.81
	95.050	C <sub>6</sub> H <sub>7</sub> O <sup>+</sup>		0.67
	107.085	C <sub>8</sub> H <sub>11</sub> <sup>+</sup>		0.26
	109.065	C <sub>7</sub> H <sub>9</sub> O <sup>+</sup>		0.36
	109.101	C <sub>8</sub> H <sub>13</sub> <sup>+</sup>		0.43
nopinone	121.102; 139.112	C <sub>9</sub> H <sub>15</sub> O <sup>+</sup>	15 <sup>d</sup> -79 <sup>c</sup>	6.5
	139.137	C <sub>10</sub> H <sub>19</sub> <sup>+</sup>		1.23
	140.114	no match		0.54
	m153	153.092	C <sub>9</sub> H <sub>13</sub> O <sub>2</sub> <sup>+</sup>	1.9 <sup>d</sup> -2.8 <sup>a</sup>
m155	155.105	C <sub>9</sub> H <sub>15</sub> O <sub>2</sub> <sup>+</sup>	0.8 <sup>a</sup> -5.3 <sup>d</sup>	0.51
m185	185.115	C <sub>10</sub> H <sub>17</sub> O <sub>3</sub> <sup>+</sup>	0.1 <sup>a</sup> -0.5 <sup>d</sup>	0.26

79 Table 3. Average night and day emission rates of birch seedlings. All reported compounds  
 80 have statistically significant emissions. Daytime light levels were 130-150  $\mu\text{mol}/\text{m}^2/\text{s}$  PAR.  
 81 Day and night temperatures in the large plant chambers were  $25.7\pm 0.1$  and  $22.0\pm 0.1$  °C,  
 82 respectively; ‘-’ corresponds to no emission at night.

Compound or m/z	Formula•H <sup>+</sup>	Night emissions, nmol/h/g $\pm$ SD	Day emissions, nmol/h/g $\pm$ SD
41.038	C <sub>3</sub> H <sub>5</sub> <sup>+</sup>	0.37 $\pm$ 0.13	0.68 $\pm$ 0.16
43.018	C <sub>2</sub> H <sub>3</sub> O <sup>+</sup>	0.64 $\pm$ 0.24	1.42 $\pm$ 0.36
43.054	C <sub>3</sub> H <sub>7</sub> <sup>+</sup>	0.14 $\pm$ 0.06	0.29 $\pm$ 0.07
45.033	C <sub>2</sub> H <sub>5</sub> O <sup>+</sup>	1.46 $\pm$ 0.64	3.35 $\pm$ 1.03
59.049	C <sub>3</sub> H <sub>7</sub> O <sup>+</sup>	1.55 $\pm$ 0.33	3.26 $\pm$ 0.89
61.029	C <sub>2</sub> H <sub>5</sub> O <sub>2</sub> <sup>+</sup>	0.20 $\pm$ 0.18	0.39 $\pm$ 0.21
63.044	C <sub>2</sub> H <sub>7</sub> O <sub>2</sub> <sup>+</sup>	0.06 $\pm$ 0.05	0.12 $\pm$ 0.06
69.070	C <sub>5</sub> H <sub>9</sub> <sup>+</sup>	-	0.15 $\pm$ 0.08
71.049	C <sub>4</sub> H <sub>7</sub> O <sup>+</sup>	0.17 $\pm$ 0.08	0.56 $\pm$ 0.29
71.085	C <sub>5</sub> H <sub>11</sub> <sup>+</sup>	-	0.08 $\pm$ 0.03
85.064	C <sub>5</sub> H <sub>9</sub> O <sup>+</sup>	-	0.23 $\pm$ 0.10
87.045	C <sub>4</sub> H <sub>7</sub> O <sub>2</sub> <sup>+</sup>	-	0.10 $\pm$ 0.03
87.081	C <sub>5</sub> H <sub>11</sub> O <sup>+</sup>	-	0.10 $\pm$ 0.04
monoterpenes	C <sub>10</sub> H <sub>17</sub> <sup>+</sup>	0.22 $\pm$ 0.29	0.69 $\pm$ 0.53

83